Journal of Polymer Research (2024) 31:51
https://doi.org/10.1007/s10965-024-03885-w

ORIGINAL PAPER

Investigation of the polymer material perforation time: comparison between two fiber laser wavelengths

Clément Romano[1] · Gunnar Ritt[1] · Michael Henrichsen[1] · Marc Eichhorn[1,2] · Christelle Kieleck[1]

Received: 2 October 2023 / Accepted: 10 January 2024

Abstract

This study investigated the perforation time of polyamide 6.6 using fiber lasers at two different wavelengths: 1070 and 1943 nm. The novelty of this research lies in the comparison of perforation times at equivalent laser irradiances on the polymer sample with two different colors of polyamide 6.6: natural and black. The results revealed that, at comparable irradiance levels and beam diameters, the 1943 nm laser source perforated the polyamide 6.6 sample faster than the 1070 nm laser source. The difference in perforation time was found to be significantly higher for natural-colored polyamide 6.6 compared to black-colored polyamide 6.6. These findings suggest that, for material processing of polyamide 6.6, especially in terms of perforation, the use of 2 µm laser sources should be privileged over 1 µm laser sources.

Keywords Polymer · Perforation · Laser

Introduction

Fiber lasers are efficient light sources that are used in many applications, including material processing. Their use is motivated by mechanical stability and vibration resistance, high beam quality and irradiance, and long lifetime. In particular, fiber lasers can be used to process various polymer materials to perform machining [1], polymer consolidation [2], transmission welding [3], perforation [4], or surface treatment [5]. These processes are performed at different laser wavelengths, mostly around 1 and 2 µm. The choice of wavelength is motivated by the availability of high-power and efficient fiber laser sources with high beam quality and the absorption of these materials at these wavelengths.

Fiber lasers emitting at 1 µm rely on ytterbium-doped fiber lasers (YDFL). At present, these are the most efficient fiber lasers sources with $>80\%$ optical-to-optical efficiencies, multi-kW output power, and a single-mode output [6]. The wavelength of 2 µm, on the other hand, relies on thulium-doped fiber lasers (TDFL). TDFLs are the second type of source that can deliver more than 1 kW of output power in a single-mode operation [7]; they can also operate with an optical-to-optical efficiency close to 60% [8].

When considering the material processing of polymers, the question of choice between 1 and 2 µm fiber lasers arises. The absorption of natural-colored plastic materials in the 2 µm region has been shown to be higher than in the 1 µm region [9, 12]. While 1 µm fiber lasers offer higher output power and greater efficiency, 2 µm lasers have the advantage of being more effectively absorbed by natural-colored polymer materials. There is a tendency in experimental studies to use 2 µm fiber lasers over 1 µm fiber lasers based on the natural absorption measurement made on polymers [10]. However, there is currently a lack of studies that directly compare the performance of these two laser wavelengths in material processing applications. Therefore, the objective of this research paper is to provide valuable insight into the performance of 1 and 2 µm fiber lasers in the context of polymer material processing. However, providing an experimental answer to this broad question would be tedious as there are too many parameters to consider, such as multiple wavelengths available from a YDFL or a TDFL, different operation modes (CW or pulsed), or irradiance levels on the polymer sample. In addition, there is a wide variety of polymer materials or processes. Thus, to perform a

✉ Clément Romano
clement.romano@iosb.fraunhofer.de

[1] Fraunhofer IOSB (Institute of Optronics, System Technologies and Image Exploitation), Gutleuthausstraße 1, 76275 Ettlingen, Germany

[2] Institute of Control Systems (IRS), Karlsruhe Institute of Technology, Fritz-Haber-Weg 1, 76131 Karlsruhe, Germany

Published online: 02 February 2024

first study we had to narrow down the number of parameters. Available lasers operating in the CW regime are often used with wavelengths of 1070 and 1943 nm. Polymer materials are typically used to replace metals in vehicles due to their lighter weight, improved impact resistance, and lower cost. For instance, in unmanned aerial vehicles, polyamide 6.6 (PA 6.6) is commonly used as it offers high strength, stiffness, and thermal resistance [11]. The absorption, reflectance, and transmission spectra of natural-colored PA 6.6 are available in the literature between 400 and 2000 nm [12]. The measurements show that the absorption increases between 1 and 2 µm while the reflectance decreases. This should give 2 µm lasers an advantage over 1 µm lasers for material processing such as cutting, perforating, or drilling. Our investigation focuses especially on the perforation time of polymer materials, a polymer process that has received little coverage in the literature. In the past, perforation of polymer materials has been reported [4], but only on reinforced polymer materials using a multi-kW multimode fiber laser at a wavelength of 1 µm.

Experimental setup

The experimental setup is depicted in Fig. 1 and is inspired by a similar experiment on polymer material perforation [4]. The collimated laser radiation from a commercial fiber laser (IPG Photonics) is launched onto the sample. The lasers had wavelengths of 1070 and 1943 nm, and were chosen based on previous experiments found in the literature on polymer material [4, 13]. Both lasers had a beam quality $M^2 < 1.1$ and a maximum output power of 290 W at 1070 nm and 200 W at 1943 nm. The 1070 nm fiber laser had a collimated beam diameter of 8.6 mm, while the 1943 nm laser had a collimated beam of 5.8 mm. To achieve a fair comparison, the 1943 nm laser beam was shaped using a telescope with two plano-convex lenses to realize a beam diameter of ~ 8 mm on the sample. Thus, both laser beams achieved a comparable irradiance up to ~ 0.8 kW/cm^2 on the sample, limited by the fiber laser power available. The irradiance was calculated using the following formula $I = 8P/\pi D^2$, where I is the irradiance, P the power, and D the gaussian beam diameter measured at $1/e^2$ of the irradiance. The laser beam diameter on the sample was measured using a beam profiling camera. Beam profile measurements, using an Ophir Pyrocam 3, were performed for both laser wavelengths up to their maximum output power. The camera was placed behind a highly reflective mirror instead of the sample to capture these measurements. This also allowed us to check that no beam deformation occurred, which could have theoretically been the result of thermal blooming [14]. For the perforation measurements, a beam dump was placed behind the sample to block further propagation of the beam once perforation was achieved. A calibrated photodiode facing the beam dump provided feedback on the transmitted power and perforation time. The laser was controlled using a trigger generator while an oscilloscope collected the data starting from the switch on time of the laser until perforation was achieved. A camera was included in the setup to monitor the sample processing safely. The sample was slightly tilted with respect to the beam propagation axis in order to prevent a potential reflection propagating back inside the laser [15]. The setup also included a fume extractor located above the sample, not shown in Fig. 1. During this experiment, two types of samples were tested:

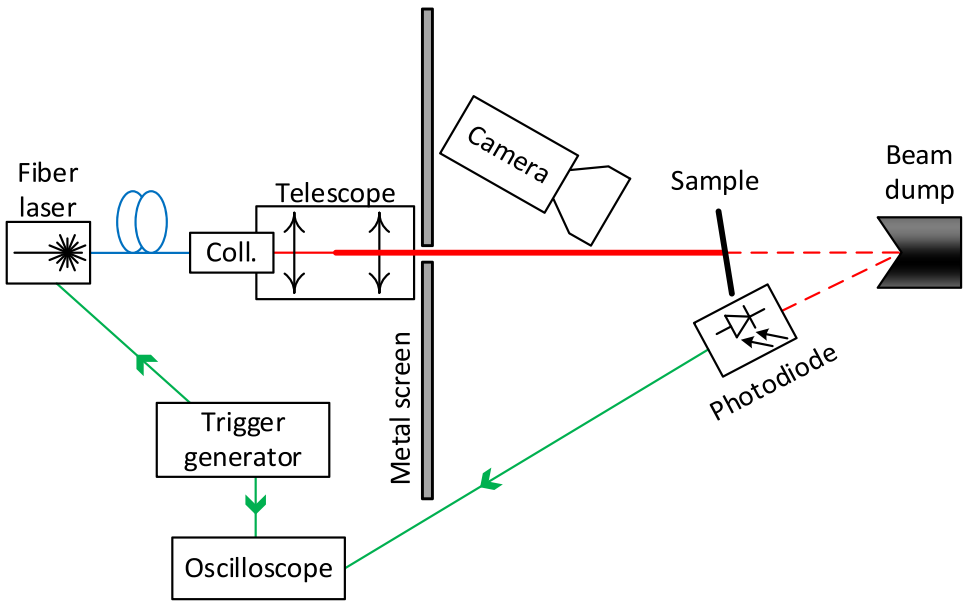

Fig. 1 Experimental setup for the investigation of the polymer perforation time

Fig. 2 Natural-colored perforated samples of PA 6.6

natural-colored and black-colored PA 6.6 (Tecamid 66). All samples had the same dimensions: $10 \times 10 \times 1$ cm^3.

In order to provide an insightful comparison between the two laser wavelengths, we conducted perforation tests at varying fiber laser output powers. This corresponded to different irradiances on the sample. For each laser power, 10 samples of PA 6.6 were perforated to provide statistics on the perforation time and thus attain a reliable value. To quantify the perforation time, we used the following definition: the perforation time corresponds to the moment when 50% of the power is initially transmitted through the sample.

Results

Figure 2 shows the results of the perforation on 10 samples of PA 6.6 with natural color. All samples were perforated by the 1943 nm fiber laser with an irradiance on sample of 0.8 kW/cm^2. It is noted that all samples look similar after exposure to the laser irradiance: a conical hole is observed with a larger diameter on the front sample side. The polymer material directly exposed to the laser radiation appears melted and carbonized. A detailed description of the various damaged areas after perforation can be found in reference [4]. An increase of the hole size with laser power could be observed over all tested samples and laser wavelengths.

Figure 3 shows some of the experimental results of transmitted power over time for different samples of natural-colored PA 6.6. The left side (respectively the right side) shows the measurement performed at a laser wavelength of 1070 nm (respectively 1943 nm) with an irradiance on the sample of 0.68 kW/cm^2 (respectively 0.8 kW/cm^2). The time scale begins with the laser switching on. The laser's activation time is negligible compared to the perforation time. Upon irradiating the sample with a 1070 nm fiber laser, some power is immediately transmitted through the sample; this is expected due to the low absorption of polymer material at the chosen wavelength. After ~ 200 s, the transmitted

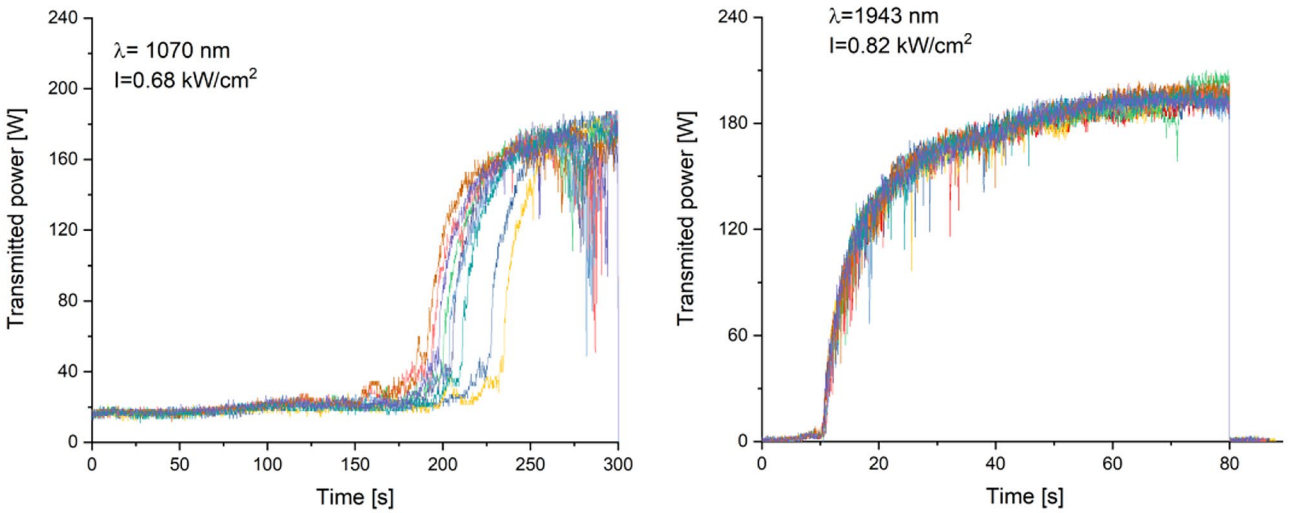

Fig. 3 Transmitted power over time for natural-colored PA 6.6

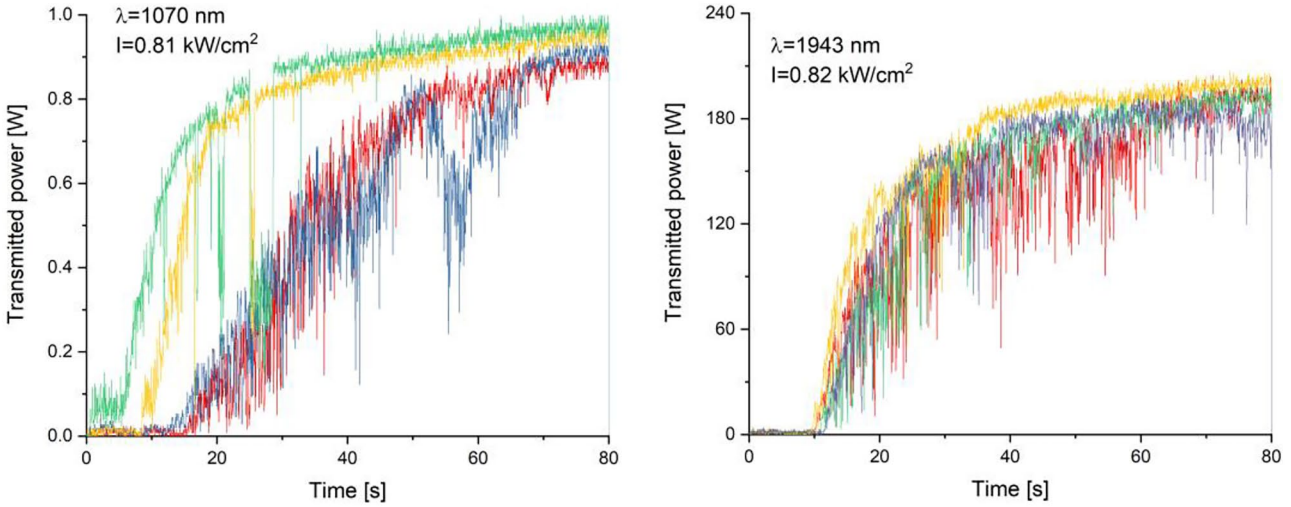

Fig. 4 Transmitted power over time for black-colored PA 6.6

power increases sharply; this corresponds to a very small hole made through the sample at the end of the perforation process. After the material is perforated, the size of the hole increases until the majority of the power is transmitted. Once the perforation is achieved and most of the power is transmitted, we observe some drops in transmission. This is attributed to material melting and dropping in the laser beam, which reduces its transmission temporarily. Smoke was also observed during the process; it traveled vertically and did not noticeably impede the laser propagation. Additional information on the process of perforating polymer materials can be found in references [4] and [16]. When irradiating the sample with a 1943 nm fiber laser, we observe that as soon as the laser switches on, no transmitted power is observed. After approximately 10 s, the first perforation of the sample is observed. The behavior is similar to the irradiance with a 1070 nm fiber laser. Comparing the two perforation measurements, better uniformity of the measurement curves is found when irradiating with a 1943 nm fiber laser.

The same measurements as those shown in Fig. 3 were performed in a second round, this time using black-colored PA 6.6. The experimental results of transmitted power over time for different samples are shown in Fig. 4 for an irradiance of 0.82 kW/cm^2 on the sample. The measurement curves follow a similar temporal evolution to the previous measurements with natural-colored PA 6.6. However, the perforation time using the 1070 nm fiber laser is much shorter than previously observed. In addition, we note that the measurement results are more chaotic than the previous results with the natural-colored PA 6.6. During the laser irradiance process, darker smoke could be observed traveling horizontally toward the laser. We believe that this behavior is the cause of the decrease in transmitted power over time [10]. This effect has already been observed and reported [4]. This indicates that the fume extractor used in the experimental setup was too weak to extract the smoke quickly enough. With the 1070 nm fiber laser, ignition of the material could sometimes be observed at irradiances of 0.82 kW/cm^2 and above. This results in a significant reduction in perforation time as illustrated by the green and yellow curves in Fig. 4 on the left side. Ignition of the sample was not observed with the 1943 nm fiber laser.

The measured average perforation times with their respective standard deviations are shown in Fig. 5. It is observed that across all cases considered, the average perforation time decreases as the laser irradiance increases. The trend of these measurements follows an exponential decreasing function. However, it should be noted that fitting these data did not yield useful physical values for predicting the perforation time beyond the studied

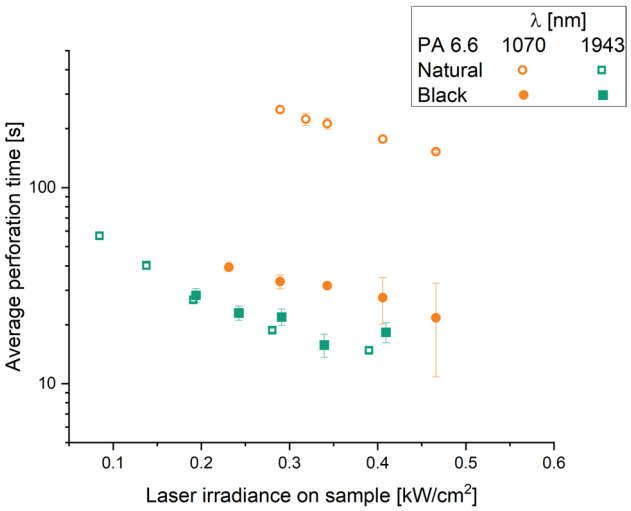

Fig. 5 Average perforation time and standard deviation versus laser irradiance on sample

range of irradiances. Regarding the 1070 nm wavelength, the perforation time shows a significant decrease, with a difference of greater than tenfold between the natural-colored and black-colored PA 6.6 samples. On the other hand, for the 1943 nm wavelength, the perforation time shows little dependency on the PA 6.6 color. Furthermore, we observed that within the tested range of irradiances, the perforation time is shorter using a 1943 nm laser source than when using a 1070 nm laser source. Regarding the natural-colored PA 6.6, the standard deviation of the perforation time demonstrates little variability and therefore is not noticeable on the figure. On the other hand, for the black-colored PA 6.6, the standard deviation is increased. This is attributed to the horizontal traveling smoke perturbating the laser propagation. For irradiances greater than 0.8 kW/cm^2 at a wavelength of 1070 nm, we note that the standard deviation increases significantly as a result of the ignition of some samples. As a result, stable perforation of the material was not achieved for these irradiances.

Conclusion

We investigated the perforation time of PA 6.6 using fiber lasers with two different wavelengths: 1070 and 1943 nm. The comparison was performed at equivalent laser irradiances on polymer samples. Two different PA 6.6 colors were investigated: natural and black. We demonstrated that at equivalent beam diameter and comparable irradiance level, a 1943 nm laser source perforates a sample of PA 6.6 significantly faster than a 1070 nm laser source. The difference in perforation time is found to be more than tenfold faster for the natural-colored PA 6.6, while for black-colored PA 6.6 the difference in perforation time is less pronounced. In conclusion, when dealing with material processing of PA 6.6, in particular the perforation of a sample, it is recommended to use 2 µm laser sources instead of 1 µm laser sources. In the future, other polymer materials and especially reinforced polymer materials will be studied to investigate wavelength-dependent effects in interaction morphology and perforation time.

Acknowledgements Funding by the German Federal Ministry of Defense and the BAAINBw is gratefully acknowledged.

Funding Open Access funding enabled and organized by Projekt DEAL.

Data availability Data underlying the results presented in this paper are not publicly available at this time but may be obtained from the authors upon reasonable request.

Declarations

Conflict interests The authors declare no conflicts of interest.

References

1. Negarestani R, Li L (2013) Fibre laser cutting of carbon fibre-reinforced polymeric composites. Proc Inst Mech Eng Part B J Eng Manuf 227(12):1755–1766. https://doi.org/10.1177/0954405413490513
2. Wittmann A, Heberle J, Huber F, Schmidt M (2021) Consolidation of thermoplastic coatings by means of a thulium-doped fiber laser. J Laser Appl 33(4):042032. https://doi.org/10.2351/7.0000501
3. Fuhrberg P, Ahrens A, Schkutow A, Frick T (2020) 2.0 µm Laser Transmission Welding. PhotonicsViews 17(2):64–68. https://doi.org/10.1002/phvs.202000013
4. Wolfrum J, Eibl S, Oeltjen E, Osterholz J, Wickert M (2021) High-energy laser effects on carbon fiber reinforced polymer composites with a focus on perforation time. J Compos Mater 55(16):2249–2262. https://doi.org/10.1177/0021998320988885
5. Scholle K et al (2018) All-fiber linearly polarized high power 2-µm single mode Tm-fiber laser for plastic processing and Ho-laser pumping applications. In Proceedings of SPIE Fiber Lasers XV: Technology and Systems, p 1051200. https://doi.org/10.1117/12.2289957
6. Nicholson JW et al (2023) Advances in mode scaling and TMI suppression in high-power fibre lasers. In: Proceedings of CLEO Europe, p 1–1. https://doi.org/10.1109/CLEO/Europe-EQEC57999.2023.10232460
7. Anderson BM, Soloman J, Flores A (2021) 1.1 kW, beam combinable thulium doped all-fiber amplifier. In: Proceedings of SPIE Fiber Lasers XVIII: Technology and Systems p 116650B. https://doi.org/10.1117/12.2576209
8. Romano C, Panitzek D, Lorenz D, Forster P, Eichhorn M, Kieleck C (2023) High-power thulium-doped fiber MOPA emitting at 2036 nm. J Light Technol 1–5. https://doi.org/10.1109/JLT.2023.3310121
9. Mingareev I, Weirauch F, Olowinsky A, Shah L, Kadwani P, Richardson M (2012) Welding of polymers using a 2 µm thulium fiber laser. Opt Laser Technol 44(7):2095–2099. https://doi.org/10.1016/j.optlastec.2012.03.020
10. Boglea A, Rösner A, Olowinsky A (2010) New perspectives for the absorber free laser welding of thermoplastics. Proceedings of ICALEO 103:567–572. https://doi.org/10.2351/1.5062082
11. Kumar A, Khanduri A, Jain P (2023) Design and development of an autonomous unmanned aerial vehicle for surface coalmines surveillance. J Phys Conf Ser 2601(1):012003. https://doi.org/10.1088/1742-6596/2601/1/012003
12. Lutey AHA, Fortunato A, Ascari A, Romoli L (2017) A modeling Approach for Plastic-Metal Laser Direct joining. Lasers Manuf Mater Process 4(3):136–151. https://doi.org/10.1007/s40516-017-0042-2
13. Schkutow A, Frick T (2016) Influence of adapted wavelengths on Temperature fields and Melt Pool geometry in laser transmission welding. Phys Procedia 83:1055–1063. https://doi.org/10.1016/j.phpro.2016.08.111
14. Frick T, Schkutow A (2018) Laser transmission welding of polymers - Irradiation strategies for strongly scattering materials, Procedia CIRP 74:538–543. https://doi.org/10.1016/j.procir.2018.08.118

15. Gebhardt M et al (2015) Impact of atmospheric molecular absorption on the temporal and spatial evolution of ultra-short optical pulses. Opt Express 23(11):13776. https://doi.org/10.1364/oe.23.013776
16. Schmitt R, Allheily V (2023) Modelling the heating of GFRP by high-energy laser radiation considering the pyrolysis of binder material. In: Proceedings of SPIE Technologies for Optical Countermeasures XIX, p 12738–5